Nanotoxicology

ISSN: 1743-5390 (Print) 1743-5404 (Online) Journal homepage: https://www.tandfonline.com/loi/inan20

Do the joint effects of size, shape and ecocorona influence the attachment and physical eco(cyto)toxicity of nanoparticles to algae?

Fazel Abdolahpur Monikh, Daniel Arenas-Lago, Petr Porcal, Renato Grillo, Peng Zhang, Zhiling Guo, Martina G. Vijver & Willie J. G. M. Peijnenburg

To cite this article: Fazel Abdolahpur Monikh, Daniel Arenas-Lago, Petr Porcal, Renato Grillo, Peng Zhang, Zhiling Guo, Martina G. Vijver & Willie J. G. M. Peijnenburg (2020) Do the joint effects of size, shape and ecocorona influence the attachment and physical eco(cyto)toxicity of nanoparticles to algae?, Nanotoxicology, 14:3, 310-325, DOI: 10.1080/17435390.2019.1692381

To link to this article: https://doi.org/10.1080/17435390.2019.1692381

NANOTOXICOLOGY
2020, VOL. 14, NO. 3, 310–325
https://doi.org/10.1080/17435390.2019.1692381

Taylor & Francis
Taylor & Francis Group

ARTICLE

Do the joint effects of size, shape and ecocorona influence the attachment and physical eco(cyto)toxicity of nanoparticles to algae?

Fazel Abdolahpur Monikh[a], Daniel Arenas-Lago[a], Petr Porcal[b], Renato Grillo[c], Peng Zhang[d], Zhiling Guo[d], Martina G. Vijver[a] and Willie J. G. M. Peijnenburg[a,e]

[a]Institute of Environmental Sciences (CML), Leiden University, Leiden, the Netherlands; [b]Institute of Hydrobiology and Soil & Water Research Infrastructure, Biology Centre CAS, České Budějovice, Czech Republic; [c]Department of Physics and Chemistry, School of Engineering, São Paulo State University (UNESP), Ilha Solteira, Brazil; [d]School of Geography, Earth and Environmental Science, University of Birmingham, Birmingham, UK; [e]Center for Safety of Substances and Products, National Institute of Public Health and the Environment (RIVM), Bilthoven, the Netherlands

ABSTRACT

We systematically investigated how the combinations of size, shape and the natural organic matter (NOM)-ecocorona of gold (Au) engineered nanoparticles (ENPs) influence the attachment of the particles to algae and physical toxicity to the cells. Spherical (10, 60 and 100 nm), urchin-shaped (60 nm), rod-shaped (10×45, 40×60 and 50×100 nm), and wire-shaped (75×500, 75×3000 and 75×6000 nm) citrate-coated and NOM-coated Au-ENPs were used. Among the spherical particles only the spherical 10 nm Au-ENPs caused membrane damage to algae. Only the rod-shaped 10×45 nm induced membrane damage among the rod-shaped Au-ENPs. Wire-shaped Au-ENPs caused no membrane damage to the algae. NOM ecocorona decreased the membrane damage effects of spherical 10 nm and rod-shaped 10×45 nm ENPs. The spherical Au-ENPs were mostly loosely attached to the cells compared to other shapes, whereas the wire-shaped Au-ENPs were mostly strongly attached compared to particles with other shapes. NOM ecocorona determined the strength of Au-ENPs attachment to the cell wall, leading to the formation of loose rather than strong attachment of Au-ENPs to the cells. After removal of the loosely and strongly attached Au-ENPs, some particles remained anchored to the surface of the algae. The highest concentration was detected for spherical 10 nm Au-ENPs followed by rod-shaped 10×45 nm Au-ENPs, while the lowest concentration was observed for the wire-shaped Au-ENPs. The combined effect of shape, size, and ecocorona controls the Au-ENPs attachment and physical toxicity to cells.

ARTICLE HISTORY
Received 16 August 2019
Revised 30 October 2019
Accepted 10 November 2019

KEYWORDS
Membrane damage; cellular association; spherical Au-ENPs; wire-shaped Au-ENPs; rod-shaped Au-ENPs

Introduction

Engineered nanoparticles (ENPs) are potentially toxic to biota (Akhil and Sudheer Khan 2017; Baun et al. 2008). Investigations on the mechanism of nanotoxicity demonstrated that ENPs could be taken up by microorganisms and induce lethal toxicity and growth inhibition, (Aruoja et al. 2009; Ji, Long, and Lin 2011; Oukarroum et al. 2012; Juganson et al. 2015; Taylor et al. 2016; Vijver et al. 2018), as well as DNA and cell damage through generation of reactive oxygen species (ROS) (He, Dorantes-Aranda, and David Waite 2012; Melegari et al. 2013; Aruoja et al. 2015). Due to their important roles in aquatic food chains as primary producer, and as a model in several guidelines and international standards for ecotoxicity testing (e.g. OECD, ISO), algal cells could be a suitable model to assess the potential toxicity of ENPs (Petit et al. 2010; Tang et al. 2018). To date, most of the studies on nanotoxicity to algae focused on chemical toxicity of ENPs, i.e. assessing whether a specific dose leads to e.g. mortality or growth inhibition. Physically induced toxicity of ENPs can also be an important pathway of nanotoxicity (Skjolding et al. 2016). For example, it was reported that graphene nanomaterials could extract phospholipids from algal cell membranes, allowing direct penetration into the cells (Zhao et al. 2017; Duan et al. 2017).

CONTACT Fazel Abdolahpur Monikh f.a.monikh@cml.leidenuniv.nl Institute of Environmental Sciences (CML), Leiden University, Van Steenis Building, Einsteinweg 2, Leiden 2333 CC, the Netherlands

Supplemental data for this article can be accessed here.

Carbon nanotubes are proposed to passively penetrate the membrane due to their needlelike shape (Zhang et al. 2018). Bhattacharya et al. (2010) showed that physical attachment of nanoplastic beads onto algal species hindered their photosynthesis, possibly through the physical blockage of light and airflow by the ENPs. Despite the higher production (in different sizes and shapes) and application of metallic ENPs compare to other types of ENPs (Vance et al. 2015), the physical toxicity of metallic ENPs is overlooked and most nanotoxicological studies are limited to assessing chemically induced toxicity. It is, for example, documented that the surfaces of silver (Ag) ENPs and zinc oxide (ZnO) ENPs can release Ag^{+} and Zn^{2+}, respectively (Navarro et al. 2008a; Miao et al. 2009; Manzo et al. 2013), and then the toxicity of these ENPs is often ascribed to the ions that are released from the particles. As a result, the toxicity of the released ions makes the differentiation between physical and chemical toxicity of metallic ENPs challenging.

Toxicity, as well as cellular uptake of ENPs by algae, were investigated with regard to differences in particle size, shape, composition and surface coating (Singh 2016; Ispas et al. 2009; Ren et al. 2017; Peng et al. 2011; Ivask et al. 2014). For example, hexametaphosphate-coated ZnO ENPs were found to be more efficiently taken up by algae than polyacrylic acid-coated particles of the same core composition and the same size (Merdzan et al. 2014). Internalization of gold (Au) and Ag ENPs coated with antibodies in cells is shown to be strongly dependent on the particle size (Jiang et al. 2008). While there are various studies about the impact of certain properties of ENPs on their toxicity, a systematic study which investigates the combined influence of size, shape and surface chemistry of ENPs, is missing in literature (Hartmann et al. 2010) despite the fact that dependencies of toxicity on different physicochemical parameters of ENPs may be strongly entangled (Xu et al. 2018).

Upon release in the environment, ENPs have been shown to interact with natural organic matter (NOM), forming so-called ecocorona on the surface of the particles (Abdolahpur Monikh et al. 2018; Arenas-Lago et al. 2019a; Grillo et al. 2015). Formation of an ecocorona occurs regardless of the surface coating of ENPs and offers a negative surface charge to ENPs (Arenas-Lago et al. 2019a). The cells, thus, 'see' the ecocorona rather than the pristine particles. The NOM ecocorona sterically and electrostatically stabilizes the particles against aggregation (Liu et al. 2013; Grillo et al. 2015). The stability of ENPs as affected by the presence of NOM may influence ENP-cell interactions, and thus the cellular toxicity (Wang et al. 2011a; Wang et al. 2011b). In addition, algae excrete various extracellular polymeric substances (EPS) into their immediate environment to retain their stable matrix structure and to create a network for cell interactions as well as to mediate their adhesion to surfaces (Xiao and Zheng 2016). EPS is the first barrier protecting the inner microorganisms against external stressors (Sheng et al. 2013; Xu et al. 2013). Previous studies reported that algae produce more EPS under the exposure to 50 mg/L copper oxide (CuO) ENPs, as a protective response to the materials (Miao et al. 2015; Hou et al. 2015). This layer, which is made up of a wide range of macromolecules such as polysaccharides, proteins, glycolipids, nucleic acids, and phospholipids, possesses a negative charge. We hypothesize that the NOM ecocorona, which has a negative charge, influences the interaction and attachment of ENPs to algal cells due to the electrostatic repulsion between the ENP-NOM ecocorona and the cells.

The objective of this study, therefore, is to systematically assess how ENP shape, size, and NOM ecocorona in conjunction influence the cellular attachment and physical (cyto)toxicity of Au-ENPs to algae. We selected Au-ENPs as the model ENPs for our study because (a) these materials could be synthesized at a wide size and shape ranges, which makes a systematic study feasible, (b) Au-ENPs are easy to be characterized by existing analytical techniques (Chithrani, Ghazani, and Chan 2006), and (c) Au-ENPs have low solubility in aquatic media (Daniel and Astruc 2004; Balasubramanian et al. 2010) which can serve to separate particle uptake from the uptake of dissolved ions.

Materials and methods

Materials

All chemicals used in this study were reagent grade. Optima grade hydrochloric acid (HCl 30%) and nitric acid (HNO_3 65%) were purchased from Merck

(Suprapure®, USA). Sodium hydroxide (NaOH) was purchased from Sigma-Aldrich (Sigma-Aldrich Corp., St. Louis, MO, USA). Suwannee River NOM was supplied by the International Humic Substances Society (1R101N). The Au-ENPs (coated with citrate) were purchased from Nanopartz™ (Nanopartz Inc., USA).

Characterization of the Au-ENPs

Transmission Electron Microscopy (JEOL 1010, TEM) operated at 70 kV was used to measure the size and to determine the shape of the Au-ENPs dispersed in Milli-Q (MQ) water. Immediately after sonication, the samples were dropped onto carbon-coated copper grids followed by evaporation of the MQ water for 1 day. The zeta potential measurements were performed using a Zetasizer Nano device (Malvern Panalytical, NL, USA). Multi-Angle Dynamic Light Scattering (MADLS) was performed using a Zetasizer Ultra (Malvern Panalytical, NL, USA) to measure the hydrodynamic size of the Au-ENPs. We have recently discussed the limitation of some light scattering techniques in the characterization of ENPs (Abdolahpur Monikh et al. 2019) of non-spherical shape ENPs. Thus, to tackle some challenges, herein we used MADLS (see the Results and Discussion). The samples were diluted using MQ water to reach a final concentration of 10 mg/L of the Au-ENPs in the dispersion to meet the detection limit of the instrument.

Incubation of Au-ENPs with NOM

A Suwannee River NOM stock solution (500 mg/L) was prepared with MQ water. The pH of the suspension was adjusted to pH 8.5 using NaOH (0.01 M). The suspension was stirred for 24 h and the pH was controlled to be maintained at the adjusted level. The NOM suspension was filtered through a 0.45 μm cellulose acetate membrane and stored at 4 °C until experimental use. For incubation of the particles with NOM to allow the ENPs and the NOM interact and form the ecocorona, aliquots of the Au-ENPs of different sizes and shapes were incubated in the filtered NOM and diluted with MQ water to reach a final concentration of 10 mg/L of Au-ENPs and 10 mg/L of NOM suspension. We selected this concentration of NOM to mimic the typical environmental NOM concentrations (Abdolahpur Monikh et al. 2018) regardless of whether this amount of NOM is sufficient to cover the particles of the different sizes and shapes equally. The concentration of the Au-ENPs was arbitrarily selected not to encounter any problems while characterizing the particles in the exposure media as described previously (Abdolahpur Monikh et al. 2019). Au-ENPs is not chemically toxic at this concentration (Chithrani, Ghazani, and Chan 2006), thus it allows us to properly investigate the physical toxicity of the ENPs. The NOM was allowed to adsorb to the surface of the particles for 24 h and the dispersion thus obtained was measured with regard to particle size and zeta potential, and used for the exposure test.

Algal cultivation and characterization

The algae *Pseudokirchinella subcapitata* was used as the test microorganism and cultivated in Woods Hole Media according to the OECD testing guideline 201 (see Section 1, SI).

Exposure testing

Along with the treatments, six samples were tested as control: three containing no NOM and Au-ENPs and three containing NOM but no Au-ENPs. Exposures were conducted in flasks by introducing a quantity of Au-ENPs from a 50 mg/L stock solution to reach a final concentration of 10 mg/L in each exposure medium. The stock solution was prepared immediately before each exposure test. A SONOPULS ultrasonicator (BANDELIN Electronic, Berlin, Germany) was used to sonicate the dispersion for 10 min at 100% amplitude. The algae were moved to autoclaved flasks to obtain a density of 2500 ± 354 cells/mL in each flask. This density was selected based on some pre-tests to facilitate the observation of the possible physical toxicity of the particles to the cells.

The algae were exposed to the citrate-coated and NOM-coated Au-ENPs in a climate chamber (22 °C) at a light intensity of 70 mE/(m^2.s) for 72 h. The stability of the Au-ENPs against dissolution and agglomeration in the exposure medium without algae cells was monitored using inductively coupled plasma mass spectrometry (ICP-MS) and MADLS, respectively. The citrate-coated and NOM-coated

Au-ENPs dispersions of different sizes and shapes were added separately to algal dispersions in flasks to obtain an exposure concentration of 10 mg/L of Au-ENPs in each flask. To reduce evaporation, the flasks were covered with cotton. The exposure was done under continuous shaking conditions at 80 rpm using a G10 Gyratory Shaker (Washington, USA), allowing to maintain optimal conditions of the algae cells as well as having the Au-ENPs as much as possible in a dispersed state. All tests were performed in triplicate.

Growth inhibition test

Although it was reported that Au-ENPs have very low toxicity, we investigated the toxicity of 10 mg/L Au-ENPs by studying the growth inhibition of the algae to assure that there is no chemical toxicity to algae. Aliquots were taken from the exposed algal suspensions at time points 0, 24, 48, and 72 h. The samples were measured using an Aquafluor Meter and a UV-Vis Spectrophotometer for the absorbance at 670-750 nm, as recommended by EPA (USEPA 1989; Rodrigues et al. 2011). The plasmon resonance of Au-ENPs in the exposure media was tested (Table S2, SI). The growth inhibition of the exposed cells was calculated with respect to untreated cells. Four different algal concentrations (1000, 5000, 7000 and 10 000 cells/mL) were measured by an Aquafluor Meter following absorbance measurement using the UV-vis spectrophotometer. The highest absorbance value was used to obtain the calibration curve of algal density (the relationship between absorbance and the counted number of cells). The calibration curve was used to measure the density of the algae after exposure to the ENPs at different sampling points. The algae density over time allows to elucidate the influence of the particles on the growth rate of the cells and to calculate the growth rates. The area under each peak of the absorbance was also measured and plotted over time.

Cell membrane damage

In this study, we used propidium iodide (PI), which is a fluorescent dye, for dying the algal cells. It is reported that PI interacts with nucleic acid macromolecules to produce red fluorescence when excited by blue light (Wang et al. 2011a). Accordingly, when the cell membrane is healthy, the PI cannot penetrate the cells and interact with the nucleic acids. However, when the cell membrane is damaged due to interaction with Au-ENPs, the PI can enter the cells and stain the nucleic acids. A PI stock solution of 1 g/L was prepared by dissolving the PI (Sigma, Cat No. F4170-10MG) into PBS and stored in darkness at 4 °C before use. The dying method was adopted from previous studies, after some modifications, (Pakrashi et al. 2013; Wang et al. 2011a) where the optimized PI staining dosage was 20 mg/L for about 2×10^6 cells. Algae exposed to the Au-ENPs (10 mg/L) were collected after 72 h of interaction. The samples were incubated with PI for 20 min and washed using PBS to remove any unbound dye. After staining, the samples were observed using a Confocal Microscope system (Leica TCS SPE) with available laser lines of 488, 532, and 633 nm. We counted a population of 1000 cells from each treatment and counted the number of cells with red fluorescence spots in this population to obtain the percentage of the damaged cells. We did not expect that the interaction between the Au-ENPs and the PI, if any, influences the cell membranes and skew the results within 20 min of incubation.

Scanning electron microscope

A JEOL 7400 F SEM operated at 6 kV of high voltage was used to picture algae in the control samples and algal cells after exposure to the Au-ENPs. The cells were observed after fixation using 2.5% glutaraldehyde in 0.2 M phosphate buffer.

Quantification of Au-ENPs loosely attached to the cell wall

After exposure, aliquots of the samples (exposed algae) from each treatment were collected and centrifuged (Sorvall RC 5B plus centrifuge, Fiberlite F21-8) at 4000 rpm for 10 min at 4 °C following the method reported previously (Arenas-Lago et al. 2019b). We removed the supernatants which were assumed to contain unbound Au-ENPs. It is also possible that some of the unbound Au-ENPs settle down due to the centrifugal force, particularly the Au-ENPs with large particle size. To minimize the concentration of the unbound particles in the

pellet, the pellet was diluted with PBS (pH 7.4) to a final volume of 10 mL, re-dispersed by shaking and centrifuged again at the same condition. This process was repeated three times. The concentration of Au in the supernatants was measured using ICP-MS as described in Section S2, SI.

Quantification of Au-ENPs strongly attached to the cell wall

Chelating agents such as ethylenediaminetetraacetic acid (EDTA) are organic molecules with two or more electron donor groups. They are capable of effectively binding polyvalent metal ions, such as Au, due to their affinity for metal ions (Flora and Pachauri 2010). The chelating potential of EDTA has been previously documented for Au-ENPs (Dozol et al. 2013). In biological or environmental media, the EDTA could bind on the one hand to ENPs and on the other hand to various chemical compounds available in the media (Bonvin et al. 2017). Herein, we used EDTA to facilitate the separation of the strongly bound Au-ENPs from the surface of the cells. In this study, the ENPs that were associated with the surface of algal cells that could not be removed using the PBS washing process referred to as strongly attached ENPs. The resulting algae suspensions from the previous steps (after removing the loosely attached Au-ENPs) were treated with 5 mL of 0.02 M EDTA for 20 min to bind the Au-ENPs, which were strongly attached to the cell walls, with the EDTA complex (Wang et al. 2011a). The concentration of the EDTA was optimized using some Pre-tests. The suspensions were vortex mixed for 10 min. The obtained suspensions were centrifuged (4000 rpm at 4 °C) for 10 min and the supernatants were separated to remove the EDTA-ENP complexes. The supernatants were used for measuring the concentration of the strongly attached Au-ENPs to the cell wall by measuring the Au concentration in the supernatant using ICP-MS.

Accumulated Au-ENPs on the algal cells

After separation of the attached Au-ENPs (loosely and strongly attached Au-ENPs) to the cell walls, the remaining algal pellets were placed into glass tubes and digested for 30–60 min with HNO_3 (65%) at 100–130 °C followed by 2 h of additional digestion with $HClO_4$ at 170 °C in an aluminum heating block. After digestion, 5 ml of MQ water was added to the residues. The total Au concentration in the resulting samples was measured using ICP-MS according to the performance condition reported in Section S2, SI. We did not differentiate between Au-ENPs internalized in the cells and Au-ENPs associated with the cells. We cannot assure that the unremoved particles after the washing processes are internalized Au-ENPs. Thus, we refer to the results of this step as Au-ENPs accumulated on the algal cells throughout this study.

Statistical analysis

Data were analyzed with the statistical program SPSS v. 19 and expressed as average ± standard deviation (SD) of three replicates. Kolmogorov-Smirnov and Levene tests were performed to check the normality and homogeneity of variances, respectively. T-test test was used to analyze statistically significant differences. All the graphs were plotted using the software OriginLab 9.1.

Results and discussion

Particle characterization

The TEM pictures of the Au-ENPs in MQ water are provided in Figure 1. The sizes and shapes of the Au-ENPs as determined by TEM were in good agreement with the information provided by the supplier. Additional TEM pictures were added to the SI (Figure S1a) to illustrate the shape of the rod-shaped particles clearly. The Au-ENPs were dispersed in MQ water and characterized in terms of particle size and zeta potential (Table 1) immediately after sonication. The attachment of the NOM ecocorona to the surface of the Au-ENPs is demonstrated by the significant variation in the zeta-potential compared to the citrate-coated Au-ENPs. The average values of the zeta potential (millivolts; mV) of about −21 to −25 mV and −28 to −32 mV were measured for the citrate-coated and NOM-coated Au-ENPs in MQ water, respectively. The zeta potential of the citrate-coated particles was significantly ($p < 0.05$) lower than the zeta potential of the NOM-coated particles. After incubation in the NOM suspension, the surface charge of the Au-ENPs shifted towards a more negative value for all the particles tested, indicating

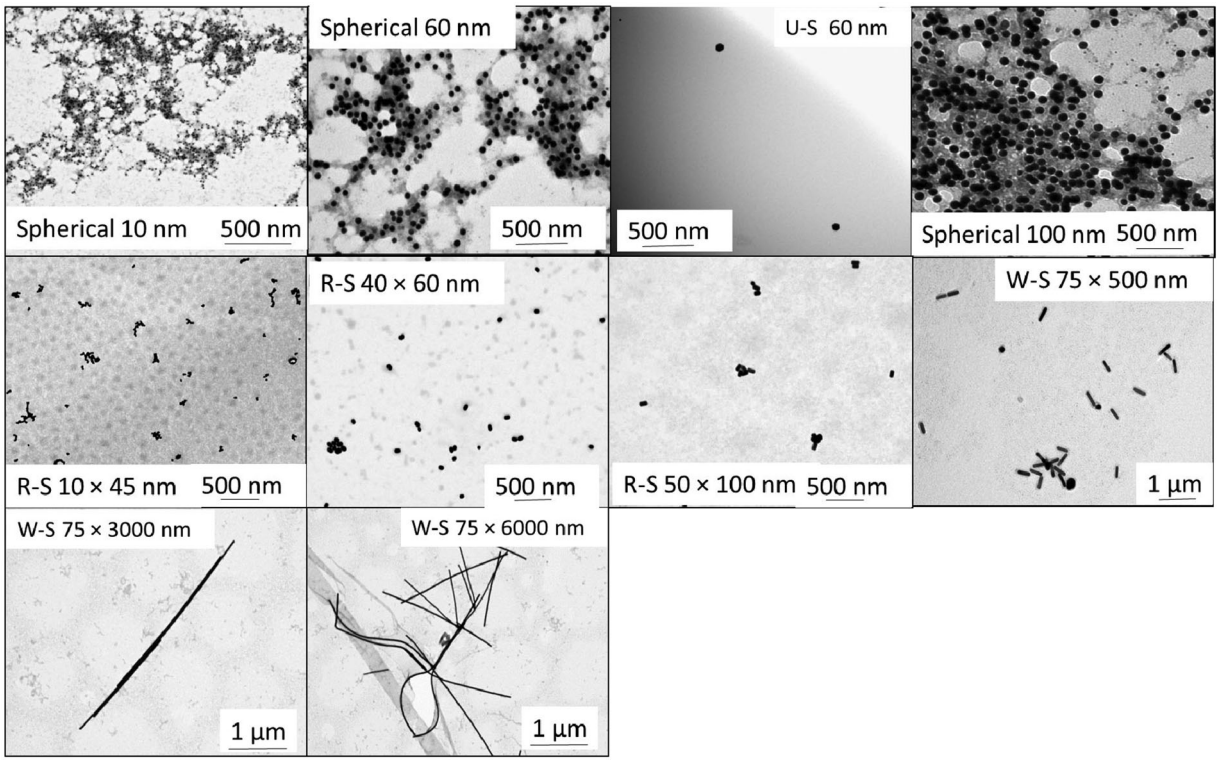

Figure 1. TEM pictures of the Au-ENPs in MQ water showing the size and shape of the Au-ENPs tested. U-S: urchin-shaped; R-S: rod-shaped and W-S: wire-shaped Au-ENPs.

Table 1. Physicochemical characterization of the citrate-coated and NOM-coated Au-ENPs used in this study.

	TEM measured size (nm)			Zeta potential (mV)		
Au-ENPs	Reported by the supplier	Measured	Surface properties	Reported by the supplier	Measured in MQ water	Measured in the exposure media
Spherical	10	10 ± 2	citrate-coated	−20	−25 ± 3	−17 ± 2
			NOM-coated		−31 ± 3	−24 ± 4
	60	60 ± 5	citrate-coated	−20	−23 ± 2	−16 ± 3
			NOM-coated		−28 ± 4	−22 ± 3
	100	100 ± 4	citrate-coated	−20	−23 ± 1	−17 ± 2
			NOM-coated		−28 ± 3	−21 ± 3
Urchin-shaped	60	60 ± 2	citrate-coated	−20	−24 ± 2	−15 ± 3
			NOM-coated		−29 ± 5	−21 ± 4
Rod-shaped	10 × 45	10 × 45 ± 2×5	citrate-coated	−22	−23 ± 1	−16 ± 3
			NOM-coated		−31 ± 3	−23 ± 2
	40 × 60	40 × 60 ± 5×7	citrate-coated	−22	−21 ± 2	−14 ± 3
			NOM-coated		−30 ± 4	−25 ± 2
	50 × 100	50 × 100 ± 6×9	citrate-coated	−20	−22 ± 3	−17 ± 4
			NOM-coated		−29 ± 5	−23 ± 3
Wire-shaped	75 × 500	75 × 500 ± 4×12	citrate-coated	−22	−22 ± 1	−15 ± 2
			NOM-coated		−30 ± 3	−24 ± 4
	75 × 3000	75 × 3074 ± 6×107	citrate-coated	−20	−21 ± 3	−15 ± 3
			NOM-coated		−32 ± 2	−22 ± 4
	75 × 6000	75 × 6102 ± 6×236	citrate-coated	−24	−23 ± 4	−16 ± 2
			NOM-coated		−29 ± 3	−22 ± 3

The table shows the measured size and zeta potential of the particles and compares them with the values reported by the supplier.
TEM measured size: size of the particles measured by transmission electron microscope, average of 500 particles. The size of the wire-shaped and rod-shaped is presented as diameter × length.

adsorption of the NOM to the Au-ENPs. The values of the zeta potential in the exposure medium increased (less negative) for both citrate-coated and NOM-coated Au-ENPs (Table 1). The mechanism of the replacement of citrate by NOM or the competition between the citrate and the NOM over the surface of the Au-ENPs was not investigated because it is out of the scope of this study.

Apart from standard properties such as hydrodynamic diameter and zeta-potential, the stability of the particles was monitored over time by measuring agglomeration rate and the dissolution rate of the Au-ENPs to assure that the observed cellular damages are not related to the released ions and chemical (cyto)toxicity. We used MADLS to measure the agglomeration rates of the Au-ENPs in the exposure medium without algal cells. Two peaks were observed for the rod-shaped and wire-shaped Au-ENPs using the MADLS which, unlike the single angle DLS, performs the measurement based on three angles (13°, 90° and 173°), offering some information about the variation of the particle shapes from a sphere. We used the highest peak to monitor the agglomeration rate of the rod-shaped and wire-shaped 75×500 nm Au-ENPs. The agglomeration rate of the wire-shaped 75×3000 nm and wire-shaped 75×6000 nm Au-ENPs could not be measured using MADLS, thus we determined it using TEM by counting 600 particles. No difference was observed between the wire-shaped 75×3000 nm and wire-shaped 75×6000 nm Au-ENPs in MQ water and those in the exposure medium. The citrate-coated and NOM-coated Au-ENPs were relatively stable (very slow agglomeration) over 72 h measurement time in the exposure medium (Figure S1b-c, SI). Due to the negative zeta potential as observed for citrate-coated and NOM-coated Au-ENPs, the particles are less prone to agglomeration and the influence of the anions and cations in the exposure medium may neutralize each other effects on the agglomeration of the Au-ENPs. This has been confirmed by the measured agglomeration rate of the citrate-coated and NOM-coated Au-ENPs in the exposure medium (Figure S1d-e, SI). Dispersed Au-ENPs would agglomerate when their surface charge is nearly neutralized, otherwise the stability against agglomeration would be achieved due to the electrostatic or steric repulsion resulting from the NOM ecocorona (Navarro et al. 2008b; Grillo et al. 2015; Arenas-Lago et al. 2019b). The dissolution rate of the particles was measured over the exposure time in the exposure medium without algae cells following the method reported by (Arenas-Lago et al. 2019b). It was found that less than 2% of the Au-ENPs were dissolved in the exposure medium. These data confirm that the culture medium did not significantly affect particle stability during the exposure time.

Algae growth inhibition

The cell size range was between 4 and 6 μm as observed by SEM (Figure S2 left, SI). The expected normal growth rate for *P. subcapitata* according to the OECD guideline 201 is 1.5-1.7 (Wilhelm et al. 2012). Algae growth in our study was similar in the control and in all the treatments with an average specific growth rate of 0.57/day to 0.7/day. In the guideline (OECD 201) the recommended initial biomass for the algae is 5×10^3-10^4. In our study, the applied initial biomass was lower than the recommended biomass which could explain the observed lower growth rate. This low growth rate was not due to the exposure to Au-ENPs as the comparison with the control confirmed this claim. We applied a lower biomass concentration for algae to facilitate investigating the physical toxicity of the particles to the cell. The concentration was selected based on previous pre-tests. The presence of NOM on the surface of the particles also did not influence the growth of the algae. These results showed that algal growth is normal after exposure to the Au-ENPs of different sizes and shapes and in the presence and absence of NOM ecocorona.

Membrane integrity

Au-ENPs may interact with the cell membrane, damage the membrane, in the first place, and then enter the cells or disrupt the functions of the membrane (Lapresta-Fernández and Blasco 2012). It was previously hypothesized that in the absence of stabilizers in the system, the high surface reactivity of ENPs results in significant cellular damage due to the acquisition of biomolecules pulled out from the cell membrane to reduce the surface free energy of the particles (Lesniak et al. 2012; Guggenheim et al. 2018). To elucidate how Au-ENPs cause cellular membrane damage to the algal cells as a function of particle size and shape and in the presence and absence of ecocorona (which plays the role of environmental stabilizer), we studied the membrane integrity of algal cells using confocal microscopy. The healthy cells were not stained owing to the intact cell membrane whereas the affected cells

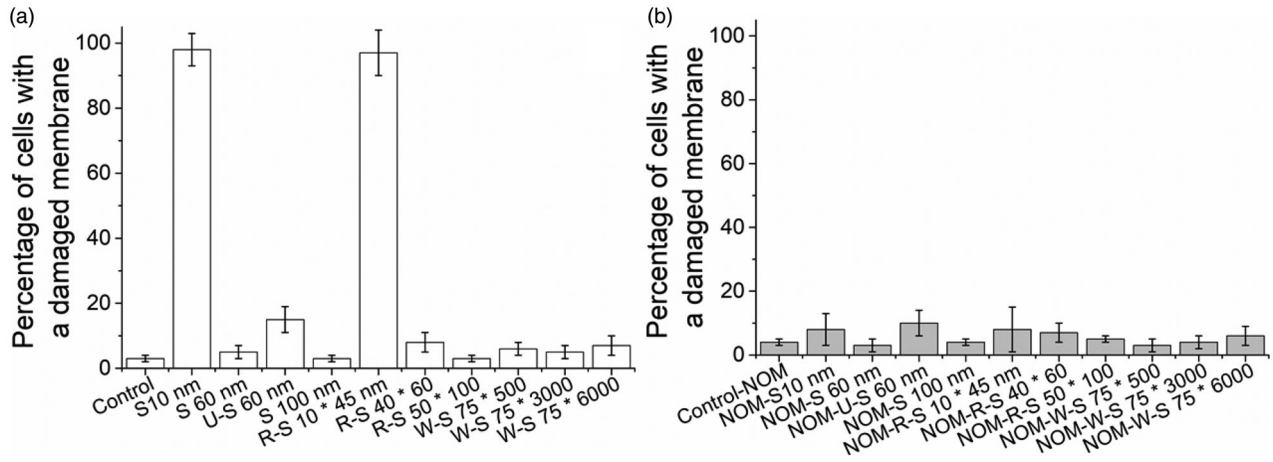

Figure 2. Confocal microscopy results show the percentage of algae with a damaged membrane after 72 h exposure to: (a) citrate-coated (S: spherical; U-S: urchin-shaped; R-S: rod-shaped; W-S: wire-shaped), and (b) NOM-coated (NOM-S: NOM-coated spherical; NOM-U-S: NOM-coated urchin-shaped; NOM-R-S: NOM-coated rod-shaped and NOM-W-S: NOM-coated wire-shaped) Au-ENPs of different sizes and shapes.

showed red fluorescence due to the uptake of the nuclear-specific stain, PI, as a result of the cell membrane damages. The results are reported in Figure 2. With regard to the citrate-coated Au-ENPs (Figure 2(a)), the highest number of cells with a damaged membrane was observed in algae exposed to spherical 10 nm and rod-shaped 10×45 nm Au-ENPs (see Figure S3, SI, red spots indicated the membrane-damaged algal cells). Considering the particle size, spherical 10 nm Au-ENPs induced membrane damage while the other spherical ENPs did not cause any significant membrane damage when compared to the control. The algae exposed to the rod-shaped 10×45 nm Au-ENPs showed the highest membrane damage compared to the other rod-shaped Au-ENPs. No membrane damage was observed as a result of the exposure to wire-shaped Au-ENPs. The damage of the membrane could be the result of direct interaction of the ENPs with the cells and subsequent acquisition of biomolecules from the cell membrane, and/or penetration of the particles into the cell wall (Malugin and Ghandehari 2010; Moreno-Garrido et al. 2015; Zhao et al. 2017). After penetrating the cell wall, Au-ENPs could interact with the phospholipid bilayer and damage the structure of the membrane bilayer. They also can trigger membrane perforation by generating and accumulating reactive oxygen species which lead to inducing oxidative stress and lipid peroxidation (Chen et al. 2019). Lipid peroxidation may increase the cell membrane permeability, leading to the loss of membrane selectivity, fluidity, and integrity (Chen et al. 2019).

We investigated whether the NOM ecocorona on the surface of the Au-ENPs would influence the observed membrane damage (Figure 2(b)). Our findings showed that the presence of NOM on the surface of the Au-ENPs decreased the ability of the spherical 10 nm and the rod-shaped 10×45 nm Au-ENPs to cause membrane damage to the cells. One explanation of this finding is that the presence of a NOM ecocorona on the surface of the ENPs might have reduced the reactivity of the ENPs by reducing the free surface energy, which consequently decreased the acquisition of biomolecules from the cell membrane by the Au-ENPs. Another explanation could be that the repulsion between the negatively charged cells and the negatively charged NOM-coated Au-ENPs decreased the interaction between the cells and the Au-ENPs. It is documented that the surfaces of algae have a high chemical affinity to positively charged ENPs (Khan et al. 2011; Moreno-Garrido et al. 2015). NOM increases the negative surface charge of the particles, thus decreasing the interaction between the ENPs and the negatively charged cell surface (Moreno-Garrido et al. 2015). The finding of this study shows that even if the ENPs cause damage to the membrane of the cells, the cells can maintain their regular growth. This may have a considerable effect on the ecological functioning of algae and their role in aquatic food chains.

Quantification of loosely attached Au-ENPs

Previous studies already showed that ENPs may attach to the surface of cells with different strengths, either strongly and/or loosely (Wang et al. 2011a; Dalai et al. 2012; Iswarya et al. 2015; Arenas-Lago et al. 2019b). In this section, we determined the loose attachment of Au-ENPs to the cell wall as a function of particle shape and size and in the presence and absence of a NOM ecocorona.

The total mass of the loosely attached Au-ENPs to the surface of the cells is reported in Figure 3(a–c). The mass of the citrate-coated and NOM-coated spherical 10 nm Au-ENPs was highest as compared to the other spherical and urchin-shaped Au-ENPs to which the cells were exposed (Figure 3(a)). The mass of the attached rod-shaped 10×45 nm was higher than the mass of the other rod-shaped Au-ENPs attached to the cells (Figure 3(b)). The mass of the wire-shaped 75×3000 nm was higher than the mass of the attached wire-shaped 75×500 nm and the wire-shaped 75×6000 nm (Figure 3(c)) Au-ENPs. The spherical Au-ENPs attached with a higher mass compared to the other shapes. The wire-shaped Au-ENPs had the lowest mass of the loosely attached particles to the surface of the cells. Higher surface attachment of smaller ENPs to the cell could be associated with the higher surface to volume ration of the smaller particles compared to the larger particles (Quigg et al. 2013).

The presence of a NOM ecocorona on the surface of the Au-ENPs increased the mass of the loosely attached particles to the cells (Figure 3(a–c)). The influence of NOM was more pronounced for smaller Au-ENPs regardless of the shape of the particles. For example, the difference between the citrate-coated and NOM-coated spherical 10 nm ENPs was significantly (*t*-test, $p < 0.0001$) higher than the difference observed for spherical 60 and 100 nm Au-ENPs (Figure 3(a)). Similarly, the presence of a NOM ecocorona on the surface of the rod-shaped 10×45 nm ENPs significantly (*t*-test, $p < 0.0001$) increased the loose attachment of the particles to the cells (Figure 3(b)).

Quantification of strongly attached Au-ENPs

The results of the quantification of the Au-ENPs which were strongly attached to the surface of the

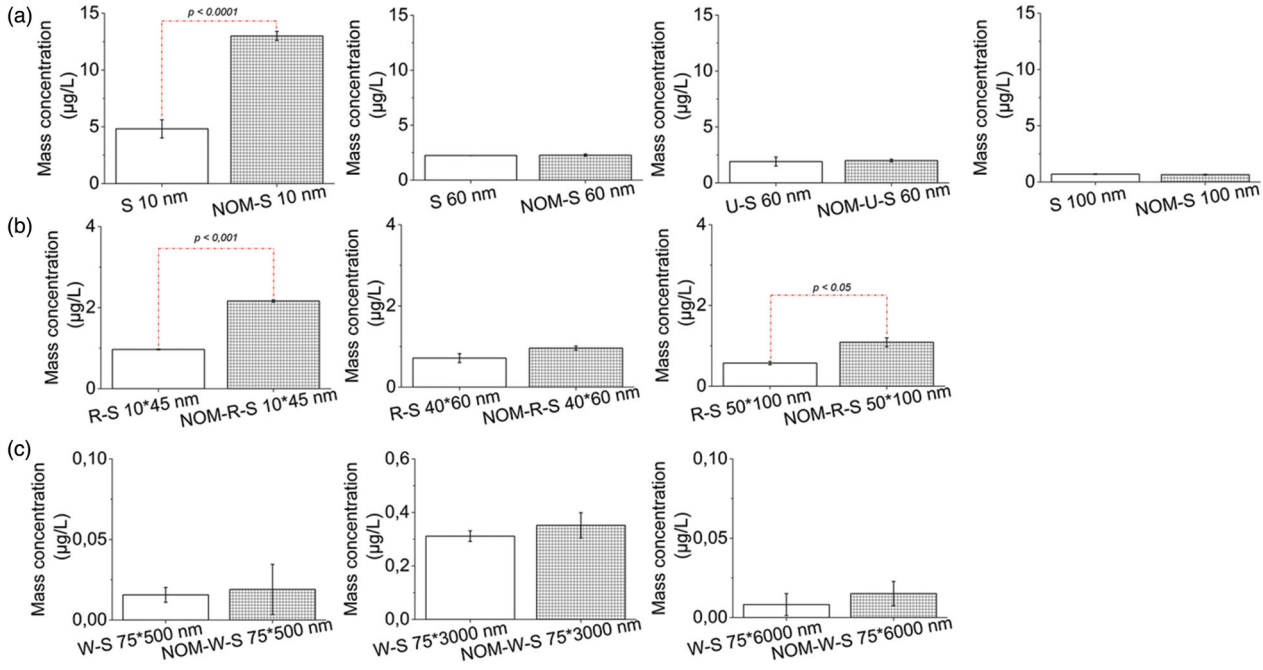

Figure 3. The measured mass concentration of the Au-ENPs which were loosely attached to the surface of the algae as a function of particle size and shape. (a) The mean mass concentration and SD of the spherical and urchin-shaped citrate-coated and NOM-coated Au-ENPs loosely attached to the surface of the cells. (b) The mean mass concentration and SD of the rod-shaped citrate-coated and NOM-coated particles loosely attached to the surface of the cells. (c) The concentration (mean and SD) of the loosely attached citrate-coated and NOM-coated wire-shaped Au-ENPs to the surface of algae.

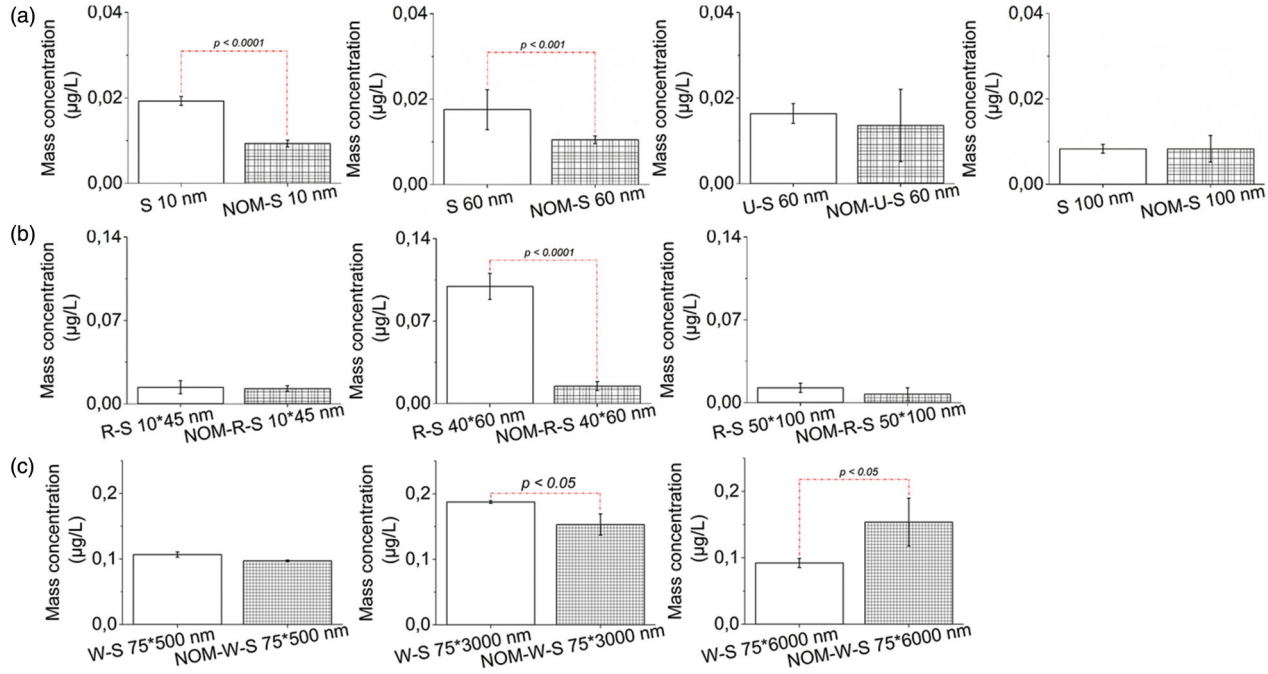

Figure 4. The measured mass and calculated number of strongly attached Au-ENPs to the surface of the algae as a function of particles size and shape. (a) The mean mass concentration and SD of the spherical and urchin-shaped citrate-coated and NOM-coated Au-ENPs. (b) The mean mass concentration and SD of the rod-shaped citrate-coated and NOM-coated particles. (c) The concentration (mean and SD) of the attached citrate-coated and NOM-coated wire-shaped particles to the surface of algae.

algal cells as a function of particle size, shape and in the presence/absence of an ecocorona, are reported in Figure 4(a–c). The data show that the pattern of attachment for strongly and loosely attached particles is different. There are no considerable differences in the mass concentration of the attached spherical and urchin-shaped Au-ENPs as size changes (Figure 4(a)). The mass of the strongly attached rod-shaped 40×60 nm Au-ENPs was higher than the mass of the other rod-shaped Au-ENPs (Figure 4(b)). Regarding the shape-based differences, wire-shaped Au-ENPs had the highest strong-attachment based on mass concentration compared to other shapes, followed by the rod-shaped Au-ENPs. The presence of NOM on the surface of the particles decreased the ability of the particles to be strongly attached to the cells, except for wire-shaped 75×6000 nm ENPs (Figure 4(a–c)). Overall, our findings showed that the presence of a NOM ecocorona on the surface of the ENPs prevents the strong attachment of Au-ENPs to cells and the particles are mostly loosely attached to the algae. As explained before, this could be attributed to the repulsion between the NOM-coated Au-ENPs and the negatively charged cells.

Quantification of accumulated Au-ENPs on the cells

Even in the presence of the protective layer of EPS, ENPs can still penetrate and subsequently be intracellularly internalized in algae (Zhao et al. 2016; Arenas-Lago et al. 2019b). However, we could not make the assumption that the remaining Au-ENPs in the pellet cells after removing the loosely and strongly attached particles, are internalized Au-ENPs. Thus, further method development is required to allow observing and quantifying the internalized particles in algae.

As the data in Figure S1d-e (SI) shows, the Au-ENPs do not dissolve in the exposure media and the dissolved fraction is not significant. Thus, obtained data is related to Au-ENPs and not to dissolved Au ions. The accumulated Au-ENPs on the algae was different between different particle shapes and sizes (Figure 5(a–c)). The amount of the accumulated Au-ENPs was also influenced in some cases by the presence of the NOM ecocorona. The accumulated spherical 10 nm ENPs were higher than spherical 60 nm > urchin-shaped 60 nm > spherical 100 nm particles (Figure 5(a)). The mass of the rod-shaped 10×45 nm ENPs was higher than for any of the other rod-shaped Au-ENPs. The mass

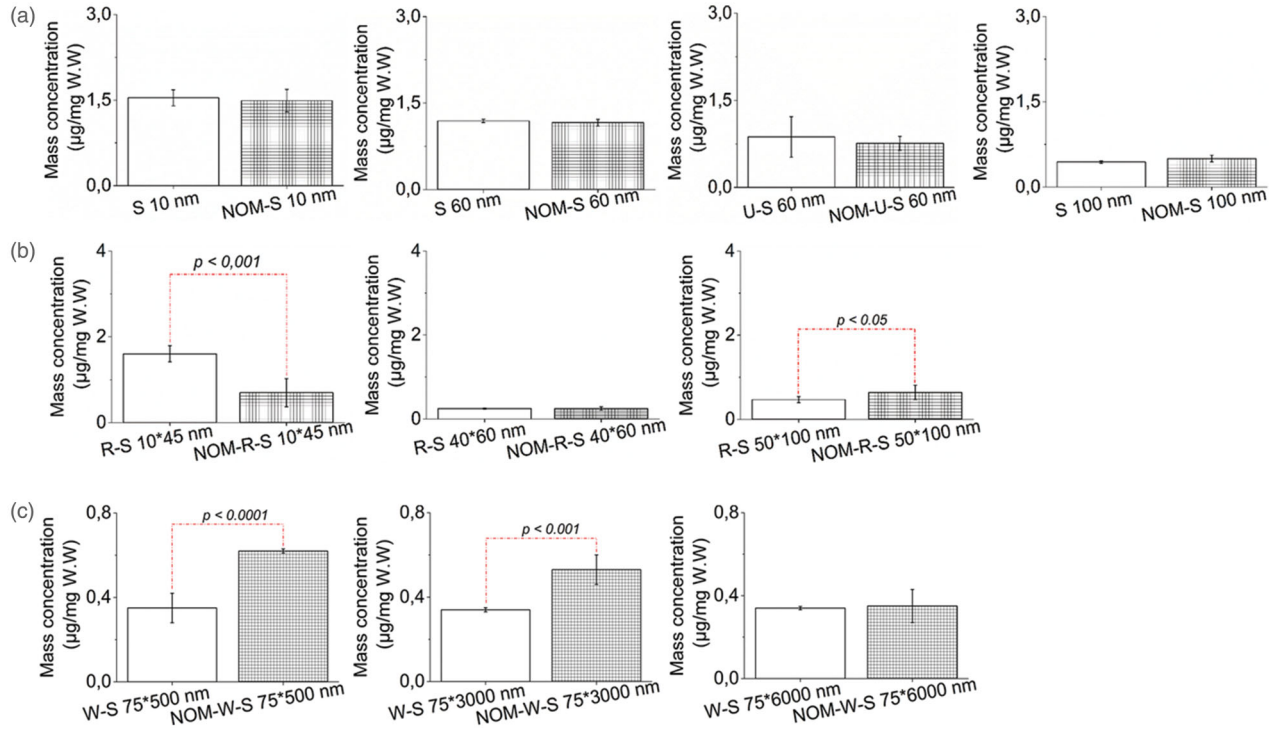

Figure 5. The measured mass of accumulated citrate-coated and NOM-coated Au-ENPs on the algae (wet weight: W.W) as a function of particle size and shape. (a) The mean mass concentration and SD of the spherical and urchin-shaped citrate-coated and NOM-coated particles. (b) The mean mass concentration and SD of the rod-shaped citrate-coated and NOM-coated particles. (c) The concentration (mean and SD) of the citrate-coated and NOM-coated wire-shaped particles.

of the rod-shaped 50×100 nm ENPs was higher than the mass of the rod-shaped 40×60 nm ENPs (Figure 5(b)). There was no significant difference between the mass of the accumulated wire-shaped Au-ENPs (Figure 5(b)). The total mass of the accumulated spherical and rod-shaped particles on the algae was higher than in the case of the wire-shaped Au-ENPs. Algae incubated with spherical 10 nm and rod-shaped 10×45 nm Au-ENPs possessed a high concentration of accumulated Au-ENPs compared to algae exposed to Au-ENPs of other shape and size.

Our results are in agreement with previous studies showing that ENPs of different sizes and shapes possess different accumulation profiles (Chithrani, Ghazani, and Chan 2006; Nel et al. 2009). In natural conditions, the accumulation of ENPs seems to resemble 'all for one and one for all'. Pores across the cell wall, which have certain diameters (5–20 nm), determine the sieving properties of a cell (Fleischer, O'Neill, and Ehwald 1999; Clements and Harris 2000; Navarro et al. 2008b). It implies that ENPs with a size smaller than the pores are expected to pass through the cell membrane. When some of the particles pass the cell wall, lipid peroxidation as induced by penetration of the particles in the cell wall may increase the cell membrane permeability and thus facilitate penetration of more particles into the membrane (Chen et al. 2019) which cannot be removed through washing processes. Moreover, the interactions of algae with ENPs might induce the formation of new pores through the surface of the algae, eventually enhancing the accumulation of the ENPs in the cell wall (Navarro et al. 2008a). This allows the penetration of ENPs across the algal cell walls. The penetration of ENPs might enlarge inherent pores, thus accelerating the ENPs accumulation in cell walls (Li et al. 2015; Sendra et al. 2017). Few studies reported that there might be a threshold radius below which cellular uptake is reduced (Decuzzi and Ferrari 2007; Nel et al. 2009). Particle sizes of about 15 to 50 nm have been suggested as the threshold for rod and spherical particles, respectively (Decuzzi and Ferrari 2007). Our findings did not support these assumptions. It is to be noted, however, that the scenario for algal cells might differ due to the differences in membrane structures between algae and mammalian cells.

The presence of NOM on the surface of the particles increased the accumulation of the Au-ENPs on

the algae in many cases (rod-shaped 50 × 100, wire-shaped 75 × 500 and wire-shaped 75 × 3000 nm Au-ENPs) and decreased it in the ceases of rod-shaped 10 × 45 nm Au-ENPs (Figure 5(a–c)). Apparently, as the size of the particles increases the NOM ecocorona increases the accumulation of Au-ENPs on algae. We suggest future studies to focus on the cell perspective on these indications to search for the reasons why NOM increases the accumulation of some particles on algae while decreasing the accumulation of other ENPs of the same type and shape.

Conclusions

Algae were exposed to citrate-coated and NOM-coated Au-ENPs of different sizes and shapes for 72 h at a concentration of 10 mg/L to elucidate the impact of a combination of different physicochemical properties on the association of the particles with algae and the physical toxicity to the cells. Confocal microscopy pictures showed that among the spherical particles the 10 nm sphere caused physical cytotoxicity to the cells by damaging the membrane. Regarding the rod-shaped particles, 10 × 45 nm Au-ENPs induced membrane damage to the algae cells, whereas none of the other particles caused any considerable membrane damage. We recommend future studies to focus more on the physical effects of ENPs, particularly needlelike particles, on microorganisms such as algae and bacteria. The ICP-MS data revealed that the mass of loosely and strongly attached Au-ENPs to the cell walls is dependent on particle size, particle shape, and presence or absence of a NOM ecocorona. The spherical 10 nm and rod-shaped 10 × 45 nm ENPs attached at the highest concentrations to the cells, as compared to all other particles investigated. The presence of a NOM ecocorona determines the strength of the attachment between the particles and the cells. Our findings showed that a NOM ecocorona caused the particles to predominantly attach loosely to the cells. Future research may focus on how the amount and type of NOM can determine the strength of the attachment. After removing the surface attached particles using washing processes, some of the Au-ENPs remained anchored to the surface of the cells. Spherical 10 nm and rod-shaped 10 × 45 nm ENPs were found to be capable of accumulating on algae in mass concentrations that were several orders of magnitude higher than for any of the other particles of different sizes and shapes. We conclude that the pattern of metallic ENPs interaction with microorganisms and their physical toxicity cannot solely be attributed to size, shape or surface chemistry, but the combined effect of physicochemical properties of the ENPs controls the final pathway through which the ENPs interact with microorganisms. Investigating the influence of each property in cellular uptake with disregard to other properties may lead to different outcomes.

Acknowledgements

The authors acknowledge the Electron Microscopy, Biology Center of CAS (LM2015062). The authors also would like to thank J. Willemse and G. Lamers (Institute of Biology Leiden University, Leiden, Netherlands) for their considerable technical assistance and the postdoctoral grant ED48 1B 2016/152-0 (Xunta de Galicia, Spain).

Disclosure statement

No potential conflict of interest was reported by the authors.

Funding

This study was financed by the H2020-MSCA-IF project BTBnano (grant agreement No. 793936).

ORCID

Fazel Abdolahpur Monikh http://orcid.org/0000-0001-9500-5303
Martina G. Vijver http://orcid.org/0000-0003-2999-1605
Willie J. G. M. Peijnenburg http://orcid.org/0000-0003-2958-9149

References

Abdolahpur Monikh, Fazel, Antonia Praetorius, Andrea Schmid, Philipp Kozin, Boris Meisterjahn, Ekaterina Makarova, Thilo Hofmann, and Frank von der Kammer. 2018. "Scientific Rationale for the Development of an OECD Test Guideline on Engineered Nanomaterial Stability." *NanoImpact* 11: 42–50. doi:10.1016/j.impact.2018.01.003.

Abdolahpur Monikh, Fazel, Latifeh Chupani, Martina G. Vijver, Marie Vancová, and Willie J.G.M. Peijnenburg. 2019. "Analytical Approaches for Characterizing and Quantifying Engineered Nanoparticles in Biological Matrices from an (Eco)Toxicological Perspective: Old Challenges, New

Methods and Techniques." *Science of the Total Environment* 660: 1283. doi:10.1016/j.scitotenv.2019.01.105.

Akhil, Khizhakkumpat., and S. Sudheer Khan. 2017. "Effect of Humic Acid on the Toxicity of Bare and Capped ZnO Nanoparticles on Bacteria, Algal and Crustacean Systems." *Journal of Photochemistry and Photobiology B: Biology* 167: 136–149. doi:10.1016/j.jphotobiol.2016.12.010.

Arenas-Lago, Daniel, Fazel Abdolahpur Monikh, Martina G. Vijver, and Willie J.G.M. Peijnenburg. 2019a. "Dissolution and Aggregation Kinetics of Zero Valent Copper Nanoparticles in (Simulated) Natural Surface Waters: Simultaneous Effects of PH, NOM and Ionic Strength." Chemosphere 226: 841–850. doi:10.1016/j.chemosphere.2019.03.190.

Arenas-Lago, Daniel, Fazel Abdolahpur Monikh, Martina G. Vijver, and Willie J.G.M. Peijnenburg. 2019b. "Interaction of Zero Valent Copper Nanoparticles with Algal Cells under Simulated Natural Conditions: Particle Dissolution Kinetics, Uptake and Heteroaggregation." *Science of the Total Environment* 689: 133–140. doi:10.1016/j.scitotenv.2019.06.388.

Arnida, Alexander Malugin, and Hamidreza Ghandehari. 2010. "Cellular Uptake and Toxicity of Gold Nanoparticles in Prostate Cancer Cells: A Comparative Study of Rods and Spheres." *Journal of Applied Toxicology* 30 (3): 212–217. doi:10.1002/jat.1486.

Aruoja, Villem, Henri Charles Dubourguier, Kaja Kasemets, and Anne Kahru. 2009. "Toxicity of Nanoparticles of CuO, ZnO and TiO2 to Microalgae *Pseudokirchneriella subcapitata*." *Science of the Total Environment* 407 (4): 1461. doi:10.1016/j.scitotenv.2008.10.053.

Aruoja, Villem, Suman Pokhrel, Mariliis Sihtmäe, Monika Mortimer, Lutz Mädler, and Anne Kahru. 2015. "Toxicity of 12 Metal-Based Nanoparticles to Algae, Bacteria and Protozoa." *Environmental Science: Nano* 2: 630–644. doi:10.1039/C5EN00057B.

Balasubramanian, Suresh K., Liming Yang, Lin Yue L. Yung, Choon Nam Ong, Wei Yi Ong, and Liya E. Yu 2010. "Characterization, Purification, and Stability of Gold Nanoparticles." *Biomaterials* 31 (34): 9023–9030. doi:10.1016/j.biomaterials.2010.08.012.

Baun, Anders., Nanna B. Hartmann, Khara D. Grieger, and Kresten Ole Kusk. 2008. "Ecotoxicity of Engineered Nanoparticles to Aquatic Invertebrates: A Brief Review and Recommendations for Future Toxicity Testing." *Ecotoxicology* 17 (5): 387. doi:10.1007/s10646-008-0208-y.

Bhattacharya, Priyanka, Sijie Lin, James P. Turner, and Pu Chun Ke. 2010. "Physical Adsorption of Charged Plastic Nanoparticles Affects Algal Photosynthesis." *Journal of Physical Chemistry C* 114 (39): 16556–16561. doi:10.1021/jp1054759.

Bonvin, Debora, Jessica A.M. Bastiaansen, Matthias Stuber, Heinrich Hofmann, and Marijana Mionić Ebersold. 2017. "Chelating Agents as Coating Molecules for Iron Oxide Nanoparticles." *RSC Advances* 7 (88): 55598. doi:10.1039/C7RA08217G.

Chen, Feiran, Zhenggao Xiao, Le Yue, Jing Wang, Yan Feng, Xiaoshan Zhu, Zhenyu Wang, and Baoshan Xing. 2019. "Algae Response to Engineered Nanoparticles: Current Understanding, Mechanisms and Implications." *Environmental Science: Nano* 6: 1026–1042. doi:10.1039/C8EN01368C.

Chithrani, B. Devika, Arezou A. Ghazani, and Warren C W. Chan. 2006. "Determining the Size and Shape Dependence of Gold Nanoparticle Uptake into Mammalian Cells." *Nano Letters* 6 (4): 662–668. doi:10.1021/nl052396o.

Dalai, Swayamprava, Sunandan Pakrashi, R. S. Suresh Kumar, N. Chandrasekaran, and Amitava Mukherjee. 2012. "A Comparative Cytotoxicity Study of TiO2 Nanoparticles under Light and Dark Conditions at Low Exposure Concentrations." *Toxicology Research* 1 (2): 116–130. doi:10.1039/c2tx00012a.

Daniel, Marie-Christine, and Didier Astruc. 2004. "Gold Nanoparticles: Assembly, Supramolecular Chemistry, Quantum-Size-Related Properties, and Applications toward Biology, Catalysis, and Nanotechnology." *Chemical Reviews* 104 (1): 293–346. doi:10.1021/cr030698+.

Decuzzi, Paolo, and Mauro Ferrari. 2007. "The Role of Specific and Non-Specific Interactions in Receptor-Mediated Endocytosis of Nanoparticles." *Biomaterials* 28 (18): 2915–2922. doi:10.1016/j.biomaterials.2007.02.013.

Dozol, Hélène, Guillaume Mériguet, Bernard Ancian, Valérie Cabuil, Haolan Xu, Dayang Wang, and Ali Abou-Hassan. 2013. "On the Synthesis of Au Nanoparticles Using EDTA as a Reducing Agent." *Journal of Physical Chemistry C* 117 (40): 20958–20966. doi:10.1021/jp4067789.

Duan, Guangxin, Yuanzhao Zhang, Binquan Luan, Jeffrey K. Weber, Royce W. Zhou, Zaixing Yang, Lin Zhao, Jiaying Xu, Judong Luo, and Ruhong Zhou. 2017. "Graphene-Induced Pore Formation on Cell Membranes." *Scientific Reports* 7: 42767. doi:10.1038/srep42767.

Fleischer, Axel, and Malcolm A. O'Neill, and Rudolf Ehwald. 1999. "The Pore Size of Non-Graminaceous Plant Cell Walls Is Rapidly Decreased by Borate Ester Cross-Linking of the Pectic Polysaccharide Rhamnogalacturonan II." *Plant Physiology*. doi:10.1104/pp.121.3.829.

Flora, Swaran J.S., and Vidhu Pachauri. 2010. "Chelation in Metal Intoxication." *International Journal of Environmental Research and Public Health* 7 (7): 2745. doi:10.3390/ijerph70.

Guggenheim, Emily J., Silvia Milani, Peter J.F. Röttgermann, Maria Dusinska, Christelle Saout, Anna Salvati, Joachim O. Rädler, and Iseult Lynch. 2018. "Refining in Vitro Models for Nanomaterial Exposure to Cells and Tissues." *NanoImpact* 10 (February): 121–142. doi:10.1016/j.impact.2018.02.008.

Grillo, R., A.H. Rosa, and L.F. Fraceto. 2015. "Engineered nanoparticles and organic matter: A review of the state-of-the-art." *Chemosphere* 119: 608–619. doi:10.1016/j.chemosphere.2014.07.049.

Hartmann, Nanna B., Frank Von der Kammer, Thilo Hofmann, Mohammed Baalousha, Stephanie Ottofuelling, and

Anders Baun. 2010. "Algal Testing of Titanium Dioxide Nanoparticles-Testing Considerations, Inhibitory Effects and Modification of Cadmium Bioavailability." *Toxicology* 269 (2-3): 190. doi:10.1016/j.tox.2009.08.008.

He, Di, Juan José Dorantes-Aranda, and T. David Waite. 2012. "Silver Nanoparticle-Algae Interactions: Oxidative Dissolution, Reactive Oxygen Species Generation and Synergistic Toxic Effects." *Environmental Science and Technology* 46 (16): 8731–8738. doi:10.1021/es300588a.

Hou, Jun, Lingzhan Miao, Chao Wang, Peifang Wang, Yanhui Ao, and Bowen Lv. 2015. "Effect of CuO Nanoparticles on the Production and Composition of Extracellular Polymeric Substances and Physicochemical Stability of Activated Sludge Flocs." *Bioresource Technology* 176: 65–70. doi:10.1016/j.biortech.2014.11.020.

Ispas, Cristina, Daniel Andreescu, Avni Patel, Dan V. Goia, Silvana Andreescu, and Kenneth N. Wallace. 2009. "Toxicity and Developmental Defects of Different Sizes and Shape Nickel Nanoparticles in Zebrafish." *Environmental Science & Technology* 43 (16): 6349–6356. doi:10.1021/es9010543.

Iswarya, Velu., M. Bhuvaneshwari, Sruthi Ann Alex, Siddharth Iyer, Gouri Chaudhuri, Prathna Thanjavur Chandrasekaran, Gopalkrishna M. Bhalerao., et al. 2015. "Combined Toxicity of Two Crystalline Phases (Anatase and Rutile) of Titania Nanoparticles towards Freshwater Microalgae: Chlorella Sp." *Aquatic Toxicology* 161: 154–169. doi:10.1016/j.aquatox.2015.02.006.

Ivask, Angela, Imbi Kurvet, Kaja Kasemets, Irina Blinova, Villem Aruoja, Sandra Suppi, Heiki Vija., et al. 2014. "Size-Dependent Toxicity of Silver Nanoparticles to Bacteria, Yeast, Algae, Crustaceans and Mammalian Cells in Vitro." *PLoS ONE* 9 (7): e102108. doi:10.1371/journal.pone.0102108.

Jiang, Wen, Betty Y.S. Kim, James T. Rutka, and Warren C.W. Chan. 2008. "Nanoparticle-Mediated Cellular Response is Size-Dependent." *Nature Nanotechnology* 3 (3): 145–150. doi:10.1038/nnano.2008.30.

Ji, Jing, Zhifeng Long, and Daohui Lin. 2011. "Toxicity of Oxide Nanoparticles to the Green Algae Chlorella Sp." *Chemical Engineering Journal* 170 (2–3): 525–530. doi:10.1016/j.cej.2010.11.026.

Juganson, Katre, Angela Ivask, Irina Blinova, Monika Mortimer, and Anne Kahru. 2015. "NanoE-Tox: New and in-Depth Database concerning Ecotoxicity of Nanomaterials." *Beilstein Journal of Nanotechnology* 6: 1788. doi:10.372/bjnano.6.183.

Khan, S. Sudheer, P. Srivatsan, N. Vaishnavi, Amitava Mukherjee, and Natarajan Chandrasekaran. 2011. "Interaction of Silver Nanoparticles (SNPs) with Bacterial Extracellular Proteins (ECPs) and Its Adsorption Isotherms and Kinetics." *Journal of Hazardous Materials* 192 (1): 299–306. doi:10.1016/j.jhazmat.2011.05.024.

Lapresta-Fernández, Alejandro, Asuncion Fernández, and Julian Blasco. 2012. "Nanoecotoxicity Effects of Engineered Silver and Gold Nanoparticles in Aquatic Organisms." *TrAC - Trends in Analytical Chemistry* 32: 40–59. doi:10.1016/j.trac.2011.09.007.

Lesniak, Anna, Federico Fenaroli, Marco P. Monopoli, Christoffer Åberg, Kenneth A. Dawson, and Anna Salvati. 2012. "Effects of the Presence or Absence of a Protein Corona on Silica Nanoparticle Uptake and Impact on Cells." *ACS Nano* 6 (7): 5845. doi:10.1021/nn300223w.

Li, Fengmin, Zhi Liang, Xiang Zheng, Wei Zhao, Miao Wu, and Zhenyu Wang. 2015. "Toxicity of Nano-TiO_2 on Algae and the Site of Reactive Oxygen Species Production." *Aquatic Toxicology* 158: 1. doi:10.1016/j.aquatox.2014.10.014.

Liu, Junfeng, Samuel Legros, Frank Von Der Kammer, and Thilo Hofmann. 2013. "Natural Organic Matter Concentration and Hydrochemistry Influence Aggregation Kinetics of Functionalized Engineered Nanoparticles." *Environmental Science & Technology* 47 (9): 4113–4120. doi:10.1021/es302447g.

Manzo, Sonia, Maria Lucia Miglietta, Gabriella Rametta, Silvia Buono, and Girolamo Di Francia. 2013. "Toxic Effects of ZnO Nanoparticles towards Marine Algae *Dunaliella tertiolecta*." *Science of the Total Environment* 445–446: 371. doi:10.1016/j.scitotenv.2012.12.051.

Melegari, Silvia Pedroso, François Perreault, Rejane Helena Ribeiro Costa, Radovan Popovic, and William Gerson Matias. 2013. "Evaluation of Toxicity and Oxidative Stress Induced by Copper Oxide Nanoparticles in the Green Alga *Chlamydomonas reinhardtii*." *Aquatic Toxicology* 142–143: 431. doi:10.1016/j.aquatox.2013.09.015.

Merdzan, Vladimir, Rute F. Domingos, Carlos E. Monteiro, Madjid Hadioui, and Kevin J. Wilkinson. 2014. "The Effects of Different Coatings on Zinc Oxide Nanoparticles and Their Influence on Dissolution and Bioaccumulation by the Green Alga, *C. reinhardtii*." *Science of the Total Environment* 488–489 (1): 316–324. doi:10.1016/j.scitotenv.2014.04.094.

Miao, Ai-Jun, Kathy A. Schwehr, Chen Xu, Sai-Jin Zhang, Zhiping Luo, Antonietta Quigg, and Peter H. Santschi. 2009. "The Algal Toxicity of Silver Engineered Nanoparticles and Detoxification by Exopolymeric Substances." *Environmental Pollution* 157 (11): 3034. doi:10.1016/j.envpol.2009.05.047.

Miao, Lingzhan, Chao Wang, Jun Hou, Peifang Wang, Yanhui Ao, Yi Li, Bowen Lv, Yangyang Yang, Guoxiang You, and Yi Xu. 2015. "Enhanced Stability and Dissolution of CuO Nanoparticles by Extracellular Polymeric Substances in Aqueous Environment." *Journal of Nanoparticle Research* 17 (10): 404. doi:10.1007/s11051-015-3208-x.

Moreno-Garrido, Ignacio, Sara Pérez, and Julián Blasco. 2015. "Toxicity of Silver and Gold Nanoparticles on Marine Microalgae." *Marine Environmental Research* 111: 60–73. doi:10.1016/j.marenvres.2015.05.008.

Navarro, Enrique, Anders Baun, Renata Behra, Nanna B. Hartmann, Juliane Filser, Ai-Jun Miao, Antonietta Quigg, Peter H. Santschi, and Laura Sigg. 2008a. "Environmental Behavior and Ecotoxicity of Engineered Nanoparticles to

Algae, Plants, and Fungi." *Ecotoxicology* 17 (5): 372. doi:10.1007/s10646-008-0214-0.

Navarro, Enrique, Flavio Piccapietra, Bettina Wagner, Fabio Marconi, Ralf Kaegi, Niksa Odzak, Laura Sigg, and Renata Behra. 2008b. "Toxicity of Silver Nanoparticles to *Chlamydomonas reinhardtii*." *Environmental Science and Technology* 42 (23): 8959–8964. doi:10.1021/es801785m.

Nel, Andre E., Lutz Mädler, Darrell Velegol, Tian Xia, Eric M.V. Hoek, Ponisseril Somasundaran, Fred Klaessig, Vince Castranova, and Mike Thompson. 2009. "Understanding Biophysicochemical Interactions at the Nano-Bio Interface." *Nature Materials* 8 (7): 543. doi:10.1038/nmat2442.

Oukarroum, Abdallah, Sébastien Bras, François Perreault, and Radovan Popovic. 2012. "Inhibitory Effects of Silver Nanoparticles in Two Green Algae, *Chlorella vulgaris* and *Dunaliella tertiolecta*." *Ecotoxicology and Environmental Safety* 78: 80. doi:10.1016/j.ecoenv.2011.11.012.

Pakrashi, Sunandan, Swayamprava Dalai, Prathna T.C, Shruti Trivedi, Radhika Myneni, Ashok M. Raichur, N. Chandrasekaran, and Amitava Mukherjee. 2013. "Cytotoxicity of Aluminium Oxide Nanoparticles towards Fresh Water Algal Isolate at Low Exposure Concentrations." *Aquatic Toxicology* 132–133: 34–45. doi:10.1016/j.aquatox.2013.01.018.

Peng, Xiaohui, Shelagh Palma, Nicholas S. Fisher, and Stanislaus S. Wong. 2011. "Effect of Morphology of ZnO Nanostructures on Their Toxicity to Marine Algae." *Aquatic Toxicology* 102 (3-4): 186. doi:10.1016/j.aquatox.2011.01.014.

Petit, Anne Noëlle, Philippe Eullaffroy, Timothée Debenest, and François Gagné. 2010. "Toxicity of PAMAM Dendrimers to *Chlamydomonas reinhardtii*." *Aquatic Toxicology* 100 (2): 187–193. doi:10.1016/j.aquatox.2010.01.019.

Quigg, Antonietta, Wei-Chun Chin, Chi-Shuo Chen, Saijin Zhang, Yuelu Jiang, Ai Jun Miao, Kathleen A. Schwehr, Chen Xu, and Peter H. Santschi. 2013. "Direct and Indirect Toxic Effects of Engineered Nanoparticles on Algae: Role of Natural Organic Matter." *ACS Sustainable Chemistry and Engineering* 1 (7): 686–702. doi:10.1021/sc400103x.

Ren, Wenting, Ruifeng Hou, Shuang Yin, Huan Yao, and Xuesong Cao. 2017. "Size-Dependent and Shape-Dependent Algal Toxicity of Aluminum Oxide Nanoparticles." In: Proceedings of the 2017 2nd International Conference on Materials Science, Machinery and Energy Engineering (MSMEE 2017). Advances in Engineering Research in Dalian, China, May 2017. doi:10.2991/msmee-17.2017.62.

Rodrigues, Lúcia Helena Ribeiro, Alexandre Arenzon, Maria Teresa Raya-Rodriguez, and Nelson Ferreira Fontoura. 2011. "Algal Density Assessed by Spectrophotometry: A Calibration Curve for the Unicellular Algae *Pseudokirchneriella subcapitata*." *Journal of Environmental Chemistry and Ecotoxicology* 3 (8): 225–228. http://www.academicjournals.org/article/article1380008244_Rodrigueset al.pdf

Sendra, Marta, M. P. Yeste, Jose Manuel Gatica, Ignacio Moreno-Garrido, and Julian Blasco. 2017. "Direct and Indirect Effects of Silver Nanoparticles on Freshwater and Marine Microalgae (*Chlamydomonas reinhardtii* and *Phaeodactylum tricornutum*)." *Chemosphere* 179: 279. doi:10.1016/j.chemosphere.2017.03.123.

Sheng, Guo Ping, Juan Xu, Hong Wei Luo, Wen Wei Li, Wei Hua Li, Han Qing Yu, Zhi Xie, Shi Qiang Wei, and Feng Chun Hu. 2013. "Thermodynamic Analysis on the Binding of Heavy Metals onto Extracellular Polymeric Substances (EPS) of Activated Sludge." *Water Research* 47 (2): 607–614. doi:10.1016/j.watres.2012.10.037.

Singh, Ashok K. 2016. "Principles of Nanotoxicology." Chapter 5 in Engineered Nanoparticles. Cambridge, MA: Academic Press. 171–227.

Skjolding, Lars Michael, Sara Nørgaard Sørensen, Nanna Bloch Hartmann, Rune Hjorth, Steffen Foss Hansen, and Anders Baun. 2016. "Aquatic Ecotoxicity Testing of Nanoparticles—the Quest to Disclose Nanoparticle Effects." *Angewandte Chemie - International Edition* 55 (49): 15224–15239. doi:10.1002/anie.201604964.

Tang, Yulin, Huaijia Xin, Feng Yang, and Xin Long. 2018. "A Historical Review and Bibliometric Analysis of Nanoparticles Toxicity on Algae." *Journal of Nanoparticle Research* 20 (4): 92. doi:10.1007/s11051-018-4196-4.

Taylor, Cameron, Marianne Matzke, Alexandra Kroll, Daniel S. Read, Claus Svendsen, and Alison Crossley. 2016. "Toxic Interactions of Different Silver Forms with Freshwater Green Algae and Cyanobacteria and Their Effects on Mechanistic Endpoints and the Production of Extracellular Polymeric Substances." *Environmental Science: Nano* 3 (2): 396–408. doi:10.1039/C5EN00183H.

United States Environmental Protection Agency. 1989. *Short term Methods for Estimating the Chronic Toxicity of Effluents and Receiving Waters to Freshwater Organisms*, edited by Weber, C.I., W.H. Peltier, T.J. Norberg-King, W.B. Horning, II, F.A. Kessler, J.R. Menkedick, T.W. Neiheisel, et al. 2nd Ed." Cincinnati, OH: U.S. Environmental Protection Agency.

Vance, Marina E., Todd Kuiken, Eric P. Vejerano, Sean P. McGinnis, Michael F. Hochella, David Rejeski, and Matthew S. Hull. 2015. "Nanotechnology in the Real World: Redeveloping the Nanomaterial Consumer Products Inventory." *Beilstein Journal of Nanotechnology* 6 (1): 1769–1780. doi:10.3762/bjnano.6.181.

Vijver, Martina G., Yujia Zhai, Zhuang Wang, and Willie J. G. M. Peijnenburg. 2018. "Emerging Investigator Series: The Dynamics of Particle Size Distributions Need to Be Accounted for in Bioavailability Modelling of Nanoparticles." *Environmental Science: Nano* 5 (11): 2473–2481. doi:10.1039/c8en00572a.

Wang, Zhenyu, Jing Li, Jian Zhao, and Baoshan Xing. 2011a. "Toxicity and Internalization of CuO Nanoparticles to Prokaryotic Alga *Microcystis aeruginosa* as Affected by Dissolved Organic Matter." *Environmental Science & Technology* 45 (14): 6032–6040. doi:10.1021/es2010573.

Wang, Zhenyu, Jing Li, Jian Zhao, and Baoshan Xing. 2011b. "Toxicity and Internalization of CuO Nanoparticles to Prokaryotic Alga Microcystis Aeruginosa as Affected by Dissolved Organic Matter." *Environmental Science and Technology* 45 (14): 6032–6040. doi:10.1021/es2010573.

Wilhelm, Klaus-Peter, and Howard I. Maibach. 2012. "OECD Guidelines for Testing of Chemicals." Dermatotoxicology, edited by Wilhelm, Klaus-Peter, Hongbo Zhai, and Howard I. Maibach, Boca Raton, FL: CRC Press.

Xiao, Rui, and Yi Zheng. 2016. "Overview of Microalgal Extracellular Polymeric Substances (EPS) and Their Applications." *Biotechnology Advances* 34 (7): 1225. doi:10.1016/j.biotechadv.2016.08.004.

Xu, Juan, Guo Ping Sheng, Ying Ma, Long Fei Wang, and Han Qing Yu. 2013. "Roles of Extracellular Polymeric Substances (EPS) in the Migration and Removal of Sulfamethazine in Activated Sludge System." *Water Research* 47 (14): 5298–5306. doi:10.4324/9780203465271.

Xu, Ming, Mahmoud G. Soliman, Xing Sun, Beatriz Pelaz, Neus Feliu, Wolfgang J. Parak, and Sijin Liu. 2018. "How Entanglement of Different Physicochemical Properties Complicates the Prediction of in Vitro and in Vivo Interactions of Gold Nanoparticles." *ACS Nano* 12 (10): 10104. doi:10.1021/acsnano.8b04906.

Zemke-White, W. L., K. D. Clements, P. J. Harris. 2000. "Acid Lysis of Macroalgae by Marine Herbivorous Fishes: Effects of Acid PH on Cell Wall Porosity." *Journal of Experimental Marine Biology and Ecology*. doi:10.1016/S0022-0981(99)00151-3.

Zhang, Luqing, Cheng Lei, Kun Yang, Jason C. White, and Daohui Lin. 2018. "Cellular Response of: *Chlorella pyrenoidosa* to Oxidized Multi-Walled Carbon Nanotubes." *Environmental Science: Nano* 5: 2415–2425. doi:10.1039/C8EN00703A.

Zhao, Jian, Xuesong Cao, Xiaoyu Liu, Zhenyu Wang, Chenchen Zhang, Jason C. White, and Baoshan Xing. 2016. "Interactions of CuO Nanoparticles with the Algae *Chlorella pyrenoidosa*: Adhesion, Uptake, and Toxicity." *Nanotoxicology* 10 (9): 1297. doi1080/17435390.2016.1206149. doi:10.1080/17435390.2016.1206149.

Zhao, Jian, Xuesong Cao, Zhenyu Wang, Yanhui Dai, and Baoshan Xing. 2017. "Mechanistic Understanding toward the Toxicity of Graphene-Family Materials to Freshwater Algae." *Water Research* 111: 18–27. doi:10.1016/j.watres.2016.12.037.